

Scaling laws in two-dimensional turbulent convection

D. Biskamp, K. Hallatschek, and E. Schwarz

Centre for Interdisciplinary Plasma Science, Max-Planck-Institut für Plasmaphysik, 85748 Garching, Germany

(Received 20 December 2000; published 22 March 2001)

Two-dimensional homogeneous turbulent convection is studied numerically. Though Bolgiano-Obukhov scaling is approximately valid, strong differences exist in the intermittency properties of velocity and temperature increments, where the latter are similar to those of a passive scalar. The main difference of the small-scale dynamics compared to a passive scalar arises from the Kelvin-Helmholtz instability, but this process does not affect the scaling properties. A condition for a scalar field to show the ramp-and-cliff structures of a passive scalar is discussed.

DOI: 10.1103/PhysRevE.63.045302

PACS number(s): 47.27.Gs, 47.27.Eq

Two-dimensional (2D) homogeneous turbulence has received considerable attention in recent years, notably in 2D hydrodynamics, e.g., [1,2], 2D magnetohydrodynamics (MHD), e.g., [3], and 2D electron magnetohydrodynamics (EMHD), e.g., [4]. Most of the interest in such systems derives from their value as paradigms in turbulence theory, which are more easily accessible to analytical and, more importantly, numerical studies than fully three-dimensional turbulence. The kinship of a two-dimensional system to its three-dimensional counterpart is strongly model dependent. While hydrodynamic turbulence differs fundamentally in two and three dimensions, 2D and 3D MHD and EMHD turbulence have very similar cascade and scaling properties. A further important turbulent system, which has been studied in 2D, is buoyancy-driven convection. Here interest is primarily focused on Rayleigh-Bénard convection in a fluid layer confined between two horizontal plates heated from below and cooled from above. In this system, however, turbulence is far from homogeneous, being dominated by boundary layer effects, e.g., [5,6]. By contrast, homogeneous convective turbulence in an open system, which we treat in this Rapid Communication, has not yet been studied intensely in the literature.

The 2D equations of thermal convection in the Boussinesq approximation can be written in terms of two functions, the vorticity $\omega = \nabla^2 \phi$, where ϕ is the stream function, $\mathbf{v} = \mathbf{e}_z \times \nabla \phi$, and the temperature fluctuation $\theta = T - T_0$,

$$\partial_t \omega + \mathbf{v} \cdot \nabla \omega + \partial_y \theta = \hat{\nu} \nabla^2 \omega, \quad (1)$$

$$\partial_t \theta + \mathbf{v} \cdot \nabla \theta = \hat{\kappa} \nabla^2 \theta + f, \quad (2)$$

where the third term on the left in Eq. (1) is the buoyancy effect, and f is the injection rate to be specified below. The equations are given in non-dimensional form using the normalizations $v t_0 / L_0 \rightarrow v$ and $\theta / T'_0 L_0 \rightarrow \theta$, where $L_0 = T_0 / T'_0$ is the temperature scale length, $t_0 = (\alpha g T'_0)^{-1/2}$ the time scale of the buoyant motion, α the thermal expansion coefficient, g the gravitational acceleration acting in $-x$ direction, in the same direction as the mean temperature gradient. We consider a quadratic box of linear size $L = 2\pi L_0$. The diffusion coefficients can be expressed in terms of the Rayleigh number $\text{Ra} = \alpha g T'_0 L^4 / \nu \kappa$ and the Prandtl number Pr

$= \nu / \kappa$, $\hat{\nu} = (2\pi)^2 (\text{Pr}/\text{Ra})^{1/2}$, $\hat{\kappa} = (2\pi)^2 / (\text{Pr Ra})^{1/2}$. We choose this normalization to the dynamic time scale t_0 instead of the more conventional one to the diffusion time, in order to underline the formal relationship of Eqs. (1) and (2) to other 2D turbulent systems such as MHD. It should be noted that our model is rather closely related to a physically realizable system: thermal convection in a magnetized plasma, which is essentially two-dimensional. The shear of the embedding magnetic field determines the size of the largest eddies excited, which can be much smaller than the average gradient scale justifying the Boussinesq approximation and the choice of periodic boundary conditions.

Two-dimensional convection is also interesting in the context of passive scalar turbulence, which has become a vividly discussed topic in turbulence theory since the seminal paper by Kraichnan [7], see, e.g., Refs. [8–11], such that the statistics of a passive scalar field θ seems to be rather well understood. It derives mainly from the spatial distribution of the field characterized by a ramp-and-cliff structure, resulting from the lagrangian distortion by the sheared velocity. Both perturbation theory (e.g., Ref. [10]) and numerical simulations (e.g., Ref. [11]) indicate that the scaling exponents ζ_p of the structure functions $S_\theta^{(p)} = \langle \delta \theta_l^p \rangle \sim l^{\zeta_p}$, $\delta \theta_l = \theta(\mathbf{x}) - \theta(\mathbf{x} - \mathbf{l})$, are strongly anomalous, in particular saturate asymptotically, $\zeta_p \rightarrow \text{const}$ for $p \rightarrow \infty$.

Whether temperature fluctuations in thermal convection behave as an active scalar or react only passively depends on the strength of the buoyancy term. This term is important at scales $l > L_{\text{BO}}$, where $L_{\text{BO}} = \epsilon_\mu^{5/4} / [\epsilon_\theta^{3/4} (g\alpha)^{3/2}]$ is the Bolgiano-Obukhov length, see Ref. [12], and ϵ_μ and ϵ_θ are the dissipation rates of kinetic energy and entropy (θ^2 can be considered as the entropy density of the system [13]). For $l < L_{\text{BO}}$ the buoyancy effect is negligible and the temperature becomes a passive scalar. In Rayleigh-Bénard convection both regimes are possible; e.g., Ref. [14]. In homogeneous turbulent convection, however, L_{BO} is always smaller than the inertial scales, since ϵ_μ decreases rapidly with μ , hence θ in Eq. (2) is always an active scalar.

The scaling properties of the scalar field depend on those of the velocity. In thermal convection both are determined selfconsistently depending only weakly on the injection process f [15], $\langle \delta v_l \delta \theta_l^2 \rangle = -\frac{4}{3} \epsilon_\theta l$, where $\delta v_l = [\mathbf{v}(\mathbf{x}) - \mathbf{v}(\mathbf{x} - \mathbf{l})] \cdot \mathbf{l} / l$, and the balance between advection and buoyancy

TABLE I. Main parameters of the simulation runs.

Run No.	N^2	n	m	$\hat{\nu}_n (= \hat{\kappa}_n)$	Ra
1	4096^2	1	3	3×10^{-5}	1.7×10^{12}
2	4096^2	2	3	2×10^{-10}	
3	4096^2	2	1	7×10^{-11}	

terms in the momentum equation (1), $\delta v_l^2/l \sim \delta \theta_l$, one obtains immediately the Bolgiano-Obukhov (BO) scaling [16,17]¹ $\delta v_l \sim l^{3/5}$, $\delta \theta_l \sim l^{1/5}$.

We solve Eqs. (1) and (2) numerically with periodic boundary conditions using a standard dealiased pseudospectral method with 4096^2 collocation points. The main parameters of the simulation runs are given in Table I. (The value of Ra is included more for curiosity, since in the case of periodic boundary conditions the physics differs from a Rayleigh-Bénard system with viscous boundary layers.) The simulations are followed for 10–15 large-eddy turnover times, which is sufficient to yield good time averages. A coherent driving f is chosen corresponding to a fixed background temperature gradient, $f = v_x = -\partial_y \phi$.² Because of the inverse cascade of the velocity a large-scale damping is required (similar to simulations of the inverse energy cascade in 2D Navier-Stokes turbulence). Hence, the dissipative terms in Eqs. (1) and (2) are replaced (in k -space) by $-(\alpha k^{-2m} + \hat{\nu}_n k^{2n})\omega_{\mathbf{k}}$ and $-(\alpha k^{-2m} + \hat{\kappa}_n k^{2n})\theta_{\mathbf{k}}$, respectively, where $\alpha = O(1)$, and we choose $m=1$ or 3 and $n=1$ or 2 . For values of n or m larger than one, dissipation is concentrated more strongly at the high- or low- k spectral edge thus broadening the inertial range, but some care has to be taken because of the tendency to generate “bottleneck” humps [18] as discussed below.

Equation (1) indicates that ω is amplified at the cliffs of θ thus forming vorticity sheets (instead of vorticity gradient sheets in 2D Navier-Stokes). These sheets suffer Kelvin-Helmholtz instability, which controls the small-scale structure of the θ cliffs in the turbulence as illustrated in Fig. 1. (The time development of the instability is faster than the dynamic distortions of the flow, such that the concept of an instability applies.) The Kelvin-Helmholtz process constitutes the main difference in the spatial behavior compared with a passive scalar shown, e.g., in Ref. [11].

The primary objective of this letter are the scaling exponents of the structure functions, which provide a rather complete picture of the statistical properties of the turbulence. (This approach has become customary in homogeneous turbulence theory, though it should be mentioned that the physical interpretation of the the set of scaling exponents is diffi-

¹Bolgiano and Obukhov derived this result assuming a stably stratified system. Its validity in the case of unstable stratification was discussed by L’vov [13].

²This driving generates a slight anisotropy of θ in the x direction as discussed in Ref. [11], in addition to a similar anisotropy of the velocity field due to the buoyancy term. However, both effects are not essential for the scaling of the structure functions given below.

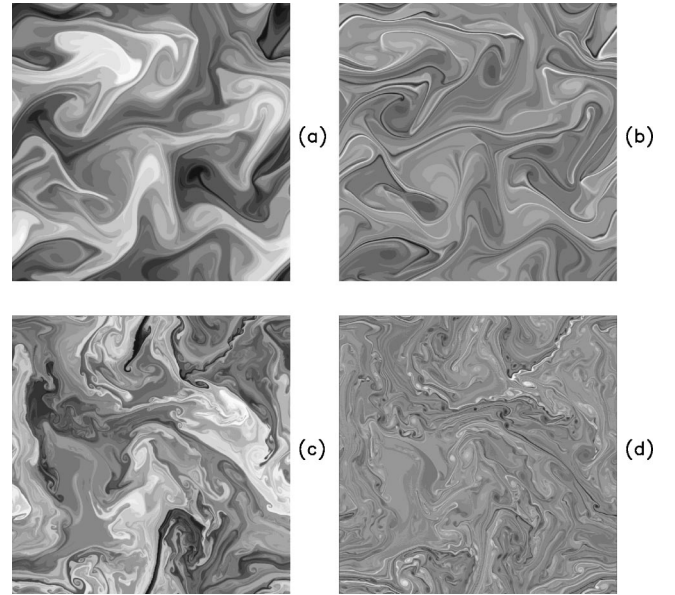


FIG. 1. Evolution of the Kelvin-Helmholtz instability in turbulent convection. Temperature (left column) and vorticity (right column) at $t=1.5$ (a),(b) and $t=3$ (c),(d).

cult, to say the least. For instance, it is not clear how to relate them to the typical spatial structures of the turbulence field.) We study, in particular, $S_v^{(p)} = \langle |\delta v_l|^p \rangle \sim l^{\xi_p}$, $S_{v\theta\theta}^{(p)} = \langle |\delta v_l \delta \theta_l^2|^{p/3} \rangle \sim l^{\zeta_p}$, which is related to the entropy flux $\mathbf{v}\theta^2$ [13], and $S_\theta^{(p)} \sim l^{\zeta_p}$. Accurate values of the scaling exponents can be obtained, even for only a short scaling range, if the fields satisfy the property of extended self-similarity (ESS) [19] and an exact relation exists to gauge the exponents. In Navier-Stokes turbulence use of ESS and Kolmogorov’s 4/5-law for $S_v^{(3)}$ allow to determine ξ_p with an uncertainty of less than 1%. In the case of thermal convection no such exact relation exists, neither for $S_v^{(p)}$ nor for $S_\theta^{(p)}$, hence the ESS property, if satisfied, determines only the relative exponents. There is, however, Yaglom’s 4/3-law mentioned above. In Fig. 2 the expression $-\langle \delta v_l \delta \theta_l^2 \rangle / (\frac{4}{3} \epsilon_\theta l)$, averaged over x

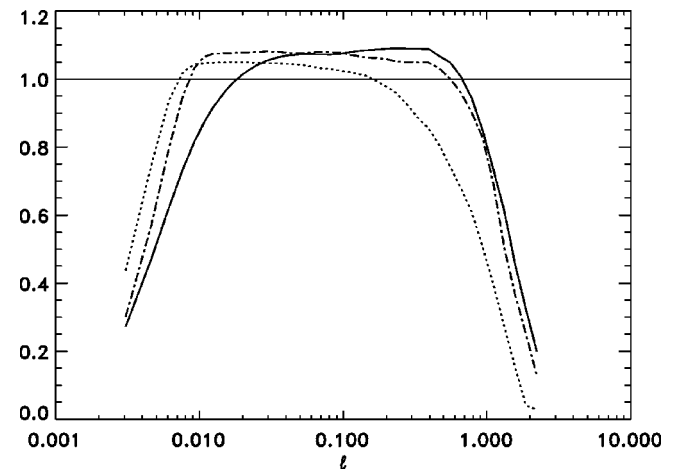


FIG. 2. Yaglom’s law $-\langle \delta v_l \delta \theta_l^2 \rangle / (\frac{4}{3} \epsilon_\theta l)$ for run 1 (continuous line), run 2 (dash-dotted line) and run 3 (dotted line).

TABLE II. Scaling exponents ζ_p and relative scaling exponents ξ_p/ξ_3 and z_p/z_3 , averaged over the three runs in Table I. The third column gives the values $\xi_p/\xi_3|_{\text{mod}}$ of model (3), the fifth column the She-Leveque exponents $z_{p,\text{SL}}$ for hydrodynamic turbulence. Only even orders p are included.

p	ξ_p/ξ_3	$\xi_p/\xi_3 _{\text{mod}}$	z_p/z_3	$z_{p,\text{SL}}$	ζ_p
2	0.68	0.69	0.71	0.70	0.39
4	1.31	1.30	1.26	1.28	0.57
6	1.92	1.88	1.73	1.78	0.66
8	2.49	2.44	2.16	2.21	0.72
10	3.05	2.98	2.57	2.59	0.76
12	3.58	3.52	2.96	2.94	0.79

and y , is plotted for the simulation runs in Table I. As can be seen, the scaling is valid over a range of $1\frac{1}{2}$ decades and the numerical value is only slightly larger than unity.

We start by considering the velocity structure functions $S_v^{(p)}$. Plotted as functions of $S_v^{(3)}$, the $S_v^{(p)}$ show perfect scalings over the entire range of the argument validating the ESS property. The relative exponents ξ_p/ξ_3 are almost identical in x and y direction and for all runs (with a scatter of 1–3%). The values show that the velocity fluctuations are only weakly intermittent, the asymptotic increase of ξ_p at large p being only slightly slower than at small p . A phenomenological model can be obtained in the framework of the log-Poisson scheme [20,21]. In Ref. [20] a general expression for the relative scaling exponents ξ_p/ξ_3 is written in terms of two parameters, β , a measure of the efficiency of energy transfer from scale to scale ($\beta=1$ in the nonintermittent limit), and Δ , which is related to the codimension C_0 of the most intermittent scales, $\Delta=C_0(1-\beta)$. Choosing $\Delta=\frac{1}{3}$ and $1-\beta=\frac{2}{3}$, which are reminiscent of the BO scaling exponents of $\delta\theta_l$ and δv_l , this expression becomes

$$\xi_p/\xi_3|_{\text{mod}} = \frac{4}{15}p + \frac{1}{3} \left[1 - \left(\frac{2}{5} \right)^{p/3} \right]. \quad (3)$$

As seen in Table II, these values fit the simulation result well, too well it seems, in fact, to be fortuitous, though we are unable to give a simple geometric interpretation. The codimension is $C_0=\frac{1}{3}$, much smaller than in 3D Navier-Stokes turbulence, hence the smallest structures are almost space-filling as can be seen in Fig. 1(d).

In contrast to the relative (ESS) exponents, the absolute values, in particular ξ_3 , are less well determined. For $m=3$, which should yield a particularly broad inertial range, a bottleneck hump appears at large scales caused by the inverse cascade of the kinetic energy in the presence of a rather abrupt transition from the inertial range to the low- k dissipative. Only for $m=1$ is this transition sufficiently gradual to avoid energy accumulation in front of the dissipation region, but this implies, of course, a shorter inertial range. From run 3 we obtain $\xi_3 \approx 1.84$, in approximate agreement with the (nonintermittent) BO value $\xi_3 = 1.8$.

Also the mixed structure functions $S_{v\theta\theta}^{(p)}$ satisfy the ESS property. (It has been argued [23] that ESS is valid for mo-

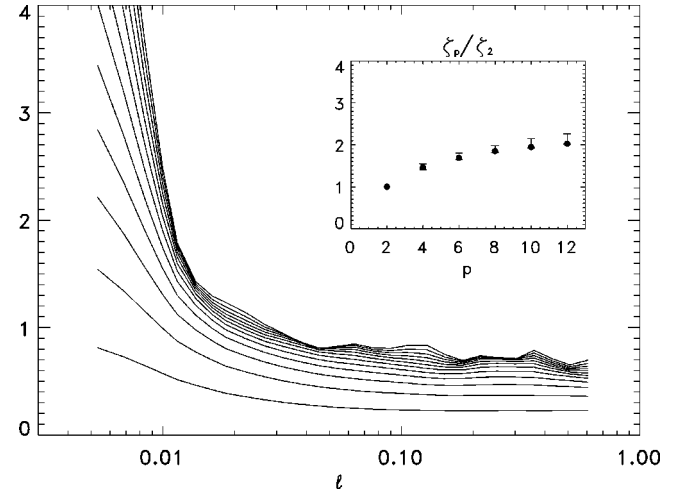


FIG. 3. $d \log S_\theta^{(p)} / d \log l$ for $p=1-12$ (from below) for run 2. The dots in the inset are the relative exponents ζ_p/ζ_2 obtained from Table II, where the error bars are obtained from Fig. 5 of Ref. [10] for a passive scalar.

ments corresponding to a convective energy flux such as $\mathbf{v}v^2$ and $\mathbf{v}\theta^2$, but not for more general quantities such as θ^3 .) Accurate values of the relative scaling exponents z_p/z_3 are obtained, which should be equal to z_p using $S_{v\theta\theta}^{(3)} \sim l$. As seen in Table II, the values are close to the She-Leveque exponents $\xi_{p,\text{SL}}$ [24] in hydrodynamic turbulence. It is, however, difficult to decide whether this agreement is significant or purely accidental, since there is no obvious reason why the statistics of the entropy flux in 2D should be more closely related to that of the kinetic energy flux in 3D than in 2D, the latter being very different as shown above. Not only the ESS functions $S_{v\theta\theta}^{(p)}(S_{v\theta\theta}^{(3)})$ but also the functions $S_{v\theta\theta}^{(p)}(l)$ themselves show rather good scaling properties at lower orders, even without taking the absolute value in the moments; see, for instance, Fig. 2.

The temperature structure functions $S_\theta^{(p)}$ do not exhibit ESS property, neither when plotted as functions of $S_\theta^{(3)}$ nor as functions of $S_{v\theta\theta}^{(3)}$, a behavior also found in experiments [23]. However the scaling quality of the $S_\theta^{(p)}$ themselves is good enough up to rather high orders $p \sim 10$ to yield accurate values of the exponents ζ_p , which are given in Table II. The $S_\theta^{(p)}$ do not show a bottleneck effect, neither at large scales, because the entropy cascade is direct, nor at small scales, the logarithmic derivative of the structure functions remaining monotonic. (By contrast, the entropy spectrum θ_k^2 exhibits a strong bottleneck effect [22], even for normal diffusion $n=1$.) The scaling range of $S_\theta^{(p)}$ is broadest in run 2. Figure 3 gives the logarithmic derivatives of $S_\theta^{(p)}$ for $p=1-12$. It should be mentioned that the instantaneous scaling exponents vary strongly in time as also found in 3D simulations of passive scalar turbulence [25], only the average over a sufficiently long period gives stationary values.

A comparison with the scaling exponents for a 2D passive scalar in [11] gives the interesting result that the relative scaling exponents ζ_p/ζ_2 agree with those of the passive scalar within error bars, as shown in the inset of Fig. 3. This behavior suggests that the scaling properties of a scalar do

not depend on the details of the velocity field, but are determined by some average properties, in our case the energy spectrum v_k^2 . (It is, however, not clear whether the relative exponents are universal. Perturbation theory [10] indicates that the passive scalar exponents depend on the velocity correlation time, which is related to the energy spectrum. In any case, for a 3D scalar field the relative exponents differ clearly from the 2D result, being less intermittent [23]. A similar tendency is found when comparing 2D and 3D MHD turbulence [26].) Figure 3 is consistent with a saturation of ζ_p . Also the probability density functions of $\delta\theta_l$ exhibit the same character as for a passive scalar, a cusp resulting from the ramp-and-cliff structure and a Gaussian at large values of the argument [8].

Finally, we briefly discuss the conditions for an active scalar to resemble a passive scalar, in particular exhibit the ramp-and-cliff spatial structure. This property depends on the character of the coupling. In the case of 2D MHD, for instance, the magnetic potential ψ , which follows an equation of the form (2), is coupled to the velocity by the non-linear Lorentz force involving the current density $\nabla^2\psi$. Here the scalar field does not show a ramp-and-cliff behavior. In 2D EMHD, where the coupling is again the Lorentz force,

the electron canonical momentum $F = \psi - d_e^2 \nabla^2 \psi$ follows Eq. (2). F has the ramp-and-cliff character at scales $l < d_e$, where $F \approx -d_e^2 \nabla^2 \psi$, but not at larger scales $l > d_e$, where $F \approx \psi$. Comparing this behavior with that of the temperature in Boussinesq convection, where the coupling occurs through the linear buoyancy term, it appears to be the absence of a higher-order derivative of the scalar field in the coupling term, not the linearity of the coupling, which gives rise to the cliffs and ramps.

In conclusion, we have studied 2D homogeneous Boussinesq turbulence. Though Bolgiano-Obukhov scaling is approximately valid, strong differences exist in the intermittency of velocity and temperature increments. While for the former intermittency is weaker than in 3D hydrodynamic turbulence, it is much stronger for the latter, similar to that of a passive scalar [11]. The main difference in the small-scale dynamics from a passive scalar arises through the Kelvin-Helmholtz instability of the vorticity sheets, but this does not seem to affect the scaling properties. In general, an active scalar shows the ramp-and-cliff structures characteristic of a passive scalar, when the coupling term in the velocity equation does not contain derivatives of the scalar.

-
- [1] G. Boffetta, A. Celani, and M. Vergassola, *Phys. Rev. E* **61**, R29 (2000).
- [2] L. Smith and V. Yakhot, *Phys. Rev. Lett.* **71**, 352 (1993).
- [3] D. Biskamp and H. Welter, *Phys. Fluids B* **1**, 1964 (1989).
- [4] D. Biskamp, E. Schwarz, A. Zeiler, A. Celani, and J.F. Drake, *Phys. Plasmas* **6**, 751 (1999).
- [5] For example, J. Werne, *Phys. Rev. E* **48**, 1020 (1993).
- [6] F. Massaioli, R. Benzi, and S. Succi, *Europhys. Lett.* **21**, 305 (1993).
- [7] R.H. Kraichnan, *Phys. Rev. Lett.* **72**, 1016 (1994).
- [8] R.H. Kraichnan, *Phys. Rev. Lett.* **78**, 4922 (1997).
- [9] U. Frisch, A. Mazzino, and M. Vergassola, *Phys. Rev. Lett.* **80**, 5532 (1998).
- [10] M. Chertkov, G. Falkovich, and V. Lebedev, *Phys. Rev. Lett.* **76**, 3707 (1996).
- [11] A. Celani, A. Lanotte, A. Mazzino, and M. Vergassola, *Phys. Rev. Lett.* **84**, 2385 (2000).
- [12] A.S. Monin and A.M. Yaglom, *Statistical Fluid Mechanics: Mechanics of Turbulence* (MIT Press, Cambridge, MA, 1975), Vol. 2.
- [13] V.S. L'vov, *Phys. Rev. Lett.* **67**, 687 (1991).
- [14] F. Chilla, S. Ciliberto, C. Innocenti, and E. Pampaloni, *Nuovo Cimento D* **D15**, 1229 (1993).
- [15] A.M. Yaglom, *Sov. Phys. Dokl.* **69**, 743 (1949).
- [16] R. Bolgiano, *J. Geophys. Res.* **64**, 2226 (1959).
- [17] A.M. Obukhov, *Sov. Phys. Dokl.* **125**, 1246 (1959).
- [18] G. Falkovich, *Phys. Fluids* **6**, 1411 (1964).
- [19] R. Benzi, S. Ciliberto, R. Tripicciono, C. Baudet, F. Massaioli, and S. Succi, *Phys. Rev. E* **48**, R29 (1993).
- [20] B. Dubrulle, *Phys. Rev. Lett.* **73**, 959 (1994).
- [21] Z.-S. She and E.C. Waymire, *Phys. Rev. Lett.* **74**, 262 (1995).
- [22] D. Biskamp, E. Schwarz, and A. Celani, *Phys. Rev. Lett.* **81**, 4855 (1998).
- [23] G. Ruiz-Chavarria, C. Baudet, and S. Ciliberto, *Physica D* **99**, 369 (1996).
- [24] Z.-S. She and E. Leveque, *Phys. Rev. Lett.* **72**, 336 (1994).
- [25] S.-J. Chen and N. Cao, *Phys. Rev. Lett.* **78**, 3459 (1997).
- [26] W.-C. Müller and D. Biskamp, *Phys. Rev. Lett.* **84**, 475 (2000).